Supporting Information

Synergistic Effect of Fluorination and Alkyl Side-Chain Engineering on Thiazole-Based Polymer Donors for Low-Cost Organic Solar Cells

Zijie Li, Ruxue Ding, Xiaobin Gu, Cai'e Zhang, Jikai Lv, Yinghui Han,* Jiahao Chen, Yunhao Cai, Xin Zhang* and Hui Huang*

Contents

1 Experimental Section

1.1 Materials and instruments

All reagents were purchased from Innochem Ltd., Bide Pharmatech Ltd., or Derthon Ltd., and used as received unless otherwise specified. The acceptor L8-BO and electron transport layer PNDIT-F3N were purchased from Solarmer Materials Inc and eFlexPV Limited, respectively. PEDOT: PSS (CLEVIOS PVP AI 4083) was provided by Heraeus.

$^{1}H/^{13}C$ NMR spectra were recorded on a JEOL JNM-ECZ500R (500 MHz) spectrometer with $CDCl_3$ and CD_2Cl_2 as solvents and tetramethylsilane as an internal reference. Electrospray ionization mass spectrometry (ESI-MS) was obtained on a Q Exactive Focus LC-MS (Thermo Scientific Company, USA). Matrix-assisted laser desorption ionization-time of flight mass spectrometry (MALDI-TOF MS) was tested by AUTOFLEX MAX, using trans-2-[3-(4-tert-Butylphenyl)-2-methyl-2-propenylidene]malononitrile (DCTB) as the matrix. Gel permeation chromatography (GPC) was performed with Agilent Technologies PL-GPC 220 at 150°C using 1,2,4-trichlorobenzene (TCB) as an eluent at the flow rate of 1.0 mL min^{-1}. Thermo-gravimetric analysis (TGA) was performed on a Q50 instrument (Shanghai Chenhua Co., Ltd.) at a heating rate of 10 °C·min^{-1} under a N_2 atmosphere. Differential scanning calorimeter (DSC) was performed on a Q2000 at a heating rate of 10 °C·min^{-1} under N_2 atmosphere.

UV–vis absorption spectra were carried out on an Agilent Cary 60 spectrometer. Electrochemical measurements were carried out under nitrogen in a deoxygenated solution of tetra-*n*-butylammonium hexafluorophosphate (0.1 M) in CH_3CN using a computer-controlled CHI600 electrochemical workstation, a glassy-carbon working electrode coated with samples, a platinum-wire auxiliary electrode, and Ag/AgCl as a reference electrode. Potentials were referenced to the ferrocenium/ferrocene ($FeCp_2^{0/+}$) couple by using ferrocene as an internal standard. According to the equations of $E_{HOMO} = -e(\varphi_{ox} + 4.8)$ (eV) and $E_{LUMO} = E_{HOMO} + E_g^{opt}$ (eV), where φ_{ox} is the onset of oxidation potential *vs.* $FeCp_2^{0/+}$, whose absolute energy level is 4.8 eV below vacuum. Grazing-incidence wide-angle X-ray scattering measurements were conducted on an Anton Paar SAXS point 5.0 system with an X-ray wavelength of 1.5418 Å and an incidence angle of 0.1°. The diffraction intensity was detected with a two-dimensional Hybrid Photon Counting detector (PILATUS3 R 1M). All X-ray measurements were performed in a vacuum environment to minimize air scattering and beam damage to samples. AFM images were obtained by Bruker Dimension Icon in the tapping mode. TEM images were obtained by HT7700Ex instrument at 110 kV accelerating voltage.

1.2 Quantum chemical calculations

All molecular structures were optimized and calculated frequencies at the B3LYP/6-31G(d) level using the Gaussian 16 program.[1] Vibrational frequency calculations were performed to check that the stable structures had no imaginary frequency. Natural bond orbital analysis was performed at the same level.[2] Track visualization were carried out by Multiwfn and VMD.[3]

1.3 Solar cell device fabrications and measurements

The solar cells were fabricated and characterized with a device configuration of ITO/PEDOT:PSS/active layer/PNDIT-F3N/Ag. After plasma cleaning for 1 min, PEDOT: PSS (Clevios P VP Al 4083) was spin-coated onto clean ITO-coated glass substrates and baked at 150 °C for 10 min. Subsequently, the substrate was transferred to the high-purity nitrogen-filled glove box. The polymer donor and L8-BO materials with D:A ratio of 1:1 were fully dissolved in chloroform (CF) at a total concentration of 14 mg/mL. The mixed solution was spin-coated on the substrate to form the active layer, followed by annealing treatment. Then, a thin layer of PNDIT-F3N was spin-coated on the films. After that, the films were transferred into a vacuum evaporator connected to the glove box. Finally, ~100 nm Ag were deposited onto the active layer sequentially by thermal evaporation at a pressure under 10^{-5} Pa.

The cells were characterized under a temperature of 25–30 °C in a glove box filled with nitrogen. The current density–voltage (*J–V*) characteristics of photovoltaic devices were obtained along the forward scan direction from –0.1 to 1 V, with a scan step of 20 mV and a dwell time of 1 ms using a Keithley 2400 source-measure unit. The photocurrent was measured under illumination simulated 100 mW cm^{-2} AM1.5G irradiation using a Newport solar simulator in an argon filled glove box. Simulator irradiance was characterized using a calibrated spectrometer and illumination intensity was set using a certified silicon diode (SRC-2020, Enlitech). External quantum efficiency (EQE) values of the devices were measured using a QE-R3011 instrument (Enli Technology Co. Ltd., Taiwan) with a scan increment of 5 nm per point.

1.4 Measurements of the hole and electron mobility by the SCLC method

The hole and electron mobility were obtained using the space charge limited current (SCLC) method. The mobility was measured with the device structure of ITO/PEDOT:PSS/J52:NFREAs/MoO_3/Ag for hole and ITO/ZnO/J52:NFREAs/PDINO/Al for electron. The hole and electron mobility was extracted by fitting the current density–voltage curves using the Mott–Gurney law,[4] Equation 1

$$J_{SCL} = 9\varepsilon\varepsilon_0\mu V^2/(8L^3) \quad (1)$$

Where J is the current density, ε_0 is the permittivity of free space, ε is the relative permittivity of the active layer, μ is the zero-field mobility, V is the voltage, and L is the film thickness.

2 Synthetic Section

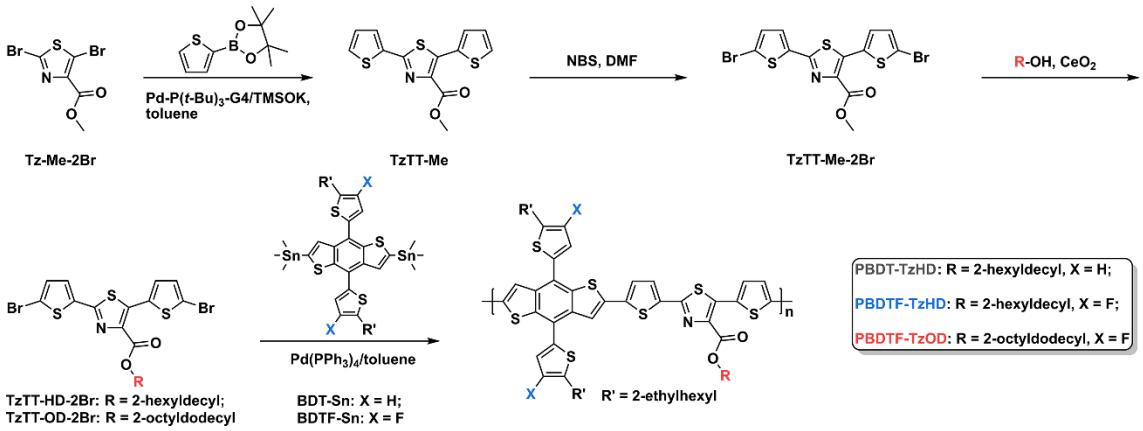

Scheme S1 Synthetic routes for PBDT-TzHD, PBDTF-TzHD, and PBDTF-TzOD.

Methyl 2,5-dibromothiazole-4-carboxylate, tributyl(thiophen-2-yl)stannane, 2-hexyldecan-1-ol, and 2-octyldodecan-1-ol were purchased from commercial sources.

Synthesis of compound TzTT-Me

A reaction flask was added methyl 2,5-dibromothiazole-4-carboxylate (500.0 mg, 1.66 mmol), 4,4,5,5-tetramethyl-2-(thiophen-2-yl)-1,3,2-dioxaborolane (766.9 mg, 3.65 mmol), Pd-P(*t*-Bu)$_3$-G4 (4.9 mg, 8.30 μmol) and TMSOK (468.3 mg, 3.65 mmol). Dry toluene (20.0 mL) was added to the mixture with a syringe under N_2 protection. The mixture was stirred at room temperature for 24 h. Afterwards, the reaction system was quenched with water. After the solution was stratified, the liquid was separated and the aqueous phase was extracted three times by dichloromethane. The organic phase was dried over anhydrous $MgSO_4$, filtered, and evaporated under reduced pressure. The crude product was purified by silica gel chromatography (petroleum ether:dichloromethane = 2:1, v/v) to give TzTT-Me as a yellow solid. (0.72 g, 71%). ^{1}H NMR (500 MHz, $CDCl_3$, δ): 7.55 (d, J = 3.7 Hz, 2H), 7.47 (dd, J = 9.1, 5.1 Hz, 2H), 7.10 (dd, J = 5.1, 3.7 Hz, 2H), 3.95 (s, 3H). ^{13}C NMR (126 MHz, $CDCl_3$, δ): 162.6, 158.9, 139.5, 139.1, 136.5, 131.4, 130.5, 129.2, 128.9, 128.1, 127.9, 127.6, 52.6. ESI MS (*m*/*z*): $[M+H]^+$, calcd. for $C_{13}H_{10}NO_2S_3^+$: 307.9795; found: 307.9868.

Synthesis of compound TzTT-Me-2Br

TzTT-Me (0.50 g, 1.63 mmol) was dissolved in DMF (20.0 mL). *N*-bromosuccinimide (726.0 mg, 4.08 mmol) was added in batches at 0 °C under darkness. The solution was allowed to slowly warm to room temperature and stirred overnight. The reaction mixture was quenched by deionized water, and then

extracted with dichloromethane. The organic phase was dried over anhydrous $MgSO_4$, filtered, and the filtrate was evaporated under reduced pressure. The crude product was purified by silica gel column chromatography (petroleum ether: dichloromethane = 5:1, v/v) to give TzTT-Me-2Br as a yellow solid product (0.59 g, 78%). ^{1}H NMR (500 MHz, CD_2Cl_2, δ): 7.25 (dd, J = 7.7, 4.0 Hz, 2H), 7.09 (d, J = 4.0 Hz, 1H), 7.06 (d, J = 4.0 Hz, 1H), 3.90 (s, 3H). ^{13}C NMR (126 MHz, $CDCl_3$, δ): 162.5, 158.0, 139.3, 138.7, 137.2, 131.8, 131.3, 131.1, 130.2, 127.9, 117.4, 117.0, 52.9. ESI MS (*m*/*z*): $[M+Na]^+$, calcd. for $C_{13}H_7Br_2NO_2S_3Na^+$: 487.7985; found: 487.7870.

Synthesis of compound TzTT-HD-2Br

A reaction flask was added TzTT-Me-2Br (0.50 g, 1.07 mmol), 2-hexyl-1-decanol (390.3 mg, 1.61 mmol), and CeO_2 (277.1 mg, 1.61 mmol), and the mixture was heated at 160ºC under N_2 atmosphere. After 48 h, the solution was cold to room temperature and the redundant 2-hexyl-1-decanol was removed by vacuum distillation. The crude product was dissolved in dichloromethane and extracted with water, and dried over anhydrous $MgSO_4$. After removing organic solvent by rotary evaporator, the crude product was purified by silica gel column chromatography (petroleum ether:dichloromethane = 10:1, v/v) to give **TzTT-HD-2Br** as a yellow oil product (0.45 g, 62%). ^{1}H NMR (500 MHz, $CDCl_3$, δ): 7.24 (d, J = 3.9 Hz, 1H), 7.18 (d, J = 3.9 Hz, 1H), 7.03 (dd, J = 7.8, 3.9 Hz, 2H), 4.23 (d, J = 6.1 Hz, 2H), 1.79-1.73 (m, 1H), 1.33-1.24 (m, 24H), 0.89-0.86 (m, 6H). ^{13}C NMR (126 MHz, $CDCl_3$, δ): 162.3, 157.6, 140.2, 137.6, 137.0, 131.9, 131.0, 130.9, 130.2, 127.7, 116.9, 116.7, 68.9, 37.4, 32.0, 32.0, 31.3, 30.1, 29.8, 29.7, 29.5, 26.8, 26.8, 22.8, 13.6. HR-MS (MALDI-TOF, *m*/*z*): $[M]^+$, calcd. for $C_{28}H_{37}Br_2NO_2S_3$: 675.033; found: 676.269.

Synthesis of compound TzTT-OD-2Br

A reaction flask was added compound 2 (0.50 g, 1.07 mmol), 2-octyldodecan-1-ol (480.7 mg, 1.61 mmol), and CeO_2 (277.1 mg, 1.61 mmol), and the mixture was heated at 160 ºC under N_2 atmosphere. After 48 h, the solution was cold to room temperature and the redundant 2-hexyl-1-decanol was removed by vacuum distillation. The crude product was dissolved in dichloromethane and extracted with water, and dried over anhydrous $MgSO_4$. After removing organic solvent by rotary evaporator, the crude product was purified by silica gel column chromatography (petroleum ether:dichloromethane = 10:1, v/v) to give compound **TzTT-OD-2Br** as a yellow oil product (0.48 g, 61%). ^{1}H NMR (500 MHz, $CDCl_3$, δ): 7.24 (d, J = 4.0 Hz, 1H), 7.18 (d, J = 4.0 Hz, 1H), 7.04 (dd, J =8.2, 4.0 Hz, 2H), 4.23 (d, J = 6.0 Hz, 2H), 1.76-1.72 (m, 1H), 1.31-1.21 (m, 32H), 0.89-0.86 (m, 6H). ^{13}C NMR (500 MHz, $CDCl_3$, δ): 162.3, 157.6, 140.6, 137.6, 137.4, 132.0, 131.0, 130.9, 130.2, 127.7, 117.0, 116.7, 68.9, 37.3, 32.1, 31.3, 30.1, 29.8, 29.8, 29.8,

29.7, 29.5, 26.8, 22.8, 15.0. HR-MS (MALDI-TOF, *m*/*z*): $[M]^+$, calcd. for $C_{32}H_{45}Br_2NO_2S_3$: 731.096; found: 731.246.

Polymerization of PBDT-TzHD

A 25 mL Schlenk flask was added into **TzTT-HD-2Br** (108.7 mg, 0.16 mmol) and (4,8-bis(5-(2-ethylhexyl)thiophen-2-yl)benzo[1,2-*b*:4,5-*b*']dithiophene-2,6-diyl)bis(trimethylstannane) (145.5 mg, 0.16 mmol). The flask was then transferred to a glovebox where anhydrous chlorobenzene (3.0 mL) and DMF (0.3 mL) was injected to dissolve the mixture. Then the $Pd(PPh_3)_4$ (9.2 mg, 8.0 μmol) was added as a catalyst, and the flask was heated at 120°C for 12 h under nitrogen. After that, 2-(tributylstannyl) thiophene and 2-bromothiophene were sequentially added to the reaction with a six hours interval. After cooling, the mixture was poured into methanol (100 mL). The precipitate was collected and further purified by Soxhlet extraction with acetone, hexane, chloroform, and chlorobenzene. The chlorobenzene fraction was then concentrated via rotavapor evaporation and precipitated in methanol. The solid was filtered and dried under vacuum to offer the final product (134.7 mg, 77%). ^{1}H NMR (500 MHz, *o*-$C_6D_4Cl_2$-*d*$_4$, δ): 7.77 (br, aromatic protons), 7.40 (br, aromatic protons), 7.09 (br, aromatic protons), 6.99 (br, aromatic protons), 4.27 (br, aliphatic protons), 2.89 (br, aliphatic protons), 1.95 (br, aliphatic protons), 1.77 (br, aliphatic protons), 1.39 (br, aliphatic protons), 1.21 (br, aliphatic protons), 0.97 (br, aliphatic protons), 0.77 (br, aliphatic protons). GPC: M_n = 38.1 kDa, M_w=64.2 kDa, PDI = 1.68.

Polymerization of PBDTF-TzHD

A 25 mL Schlenk flask was added into **TzTT-HD-2Br** (114.6 mg, 0.17 mmol) and (4,8-bis(5-(2-ethylhexyl)-4-fluorothiophen-2-yl)benzo[1,2-*b*:4,5-*b*']dithiophene-2,6-diyl)bis(trimethylstannane) (159.5 mg, 0.17 mmol). The flask was then transferred to a glovebox where anhydrous chlorobenzene (3.0 mL) and DMF (0.3 mL) was injected to dissolve the mixture. Then the $Pd(PPh_3)_4$ (9.8 mg, 8.5 μmol) was added as a catalyst, and the flask was heated at 120 °C for 12 h under nitrogen. After that, 2-(tributylstannyl) thiophene and 2-bromothiophene were sequentially added to the reaction with a six hours interval. After cooling, the mixture was poured into methanol (100 mL). The precipitate was collected and further purified by Soxhlet extraction with acetone, hexane, chloroform, and chlorobenzene. The chlorobenzene fraction was then concentrated via rotavapor evaporation and precipitated in methanol. The solid was filtered and dried under vacuum to offer the final product (174.0 mg, yield 91%). ^{1}H NMR (500 MHz, *o*-$C_6D_4Cl_2$-*d*$_4$, δ): 7.80 (br, aromatic protons), 7.29 (br, aromatic protons), 7.08 (br, aromatic protons), 6.98 (br, aromatic protons), 4.26 (br, aliphatic protons), 3.00 (br, aliphatic protons), 1.97 (br, aliphatic protons), 1.71 (br, aliphatic protons), 1.21 (br, aliphatic protons), 0.78 (br, aliphatic protons).

GPC: M_n = 41.6 kDa, M_w=67.0 kDa, PDI = 1.61.

Polymerization of PBDTF-TzOD

A 25 mL Schlenk flask was added into **TzTT-OD-2Br** (77.6 mg, 0.11 mmol) and (4,8-bis(5-(2-ethylhexyl)-4-fluorothiophen-2-yl)benzo[1,2-*b*:4,5-*b*']dithiophene-2,6-diyl)bis(trimethylstannane) (99.7 mg, 0.11 mmol). The flask was then transferred to a glovebox where anhydrous chlorobenzene (2.0 mL) and DMF (0.2 mL) was injected to dissolve the mixture. Then the $Pd(PPh_3)_4$ (6.4 mg, 5.5 μmol) was added as a catalyst, and the flask was heated at 120 ^oC for 12 h under nitrogen. After that, 2-(tributylstannyl) thiophene and 2-bromothiophene were sequentially added to the reaction with a six hours interval. After cooling, the mixture was poured into methanol (100 mL). The precipitate was collected and further purified by Soxhlet extraction with acetone, hexane, chloroform, and chlorobenzene. The chlorobenzene fraction was then concentrated via rotavapor evaporation and precipitated in methanol. The solid was filtered and dried under vacuum to offer the final product (86.2 mg, yield 69%). ^{1}H NMR (500 MHz, *o*-$C_6D_4Cl_2$-d_4, δ): 7.81 (br, aromatic protons), 7.30 (br, aromatic protons), 7.08 (br, aromatic protons), 6.98 (br, aromatic protons), 4.28 (br, aliphatic protons), 2.85 (br, aliphatic protons), 1.97 (br, aliphatic protons), 1.68 (br, aliphatic protons), 1.39 (br, aliphatic protons), 1.21 (br, aliphatic protons), 0.94 (br, aliphatic protons), 0.78 (br, aliphatic protons). GPC: M_n = 44.9 kDa, M_w=83.1 kDa, PDI = 1.85.

3 Supporting Figures

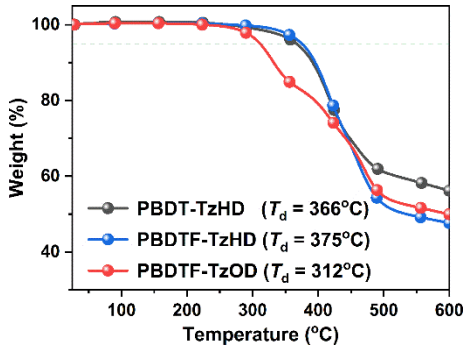

Figure S1 Thermogravimetric analysis for **PBDT-TzHD**, **PBDTF-TzHD**, and **PBDTF-TzOD**.

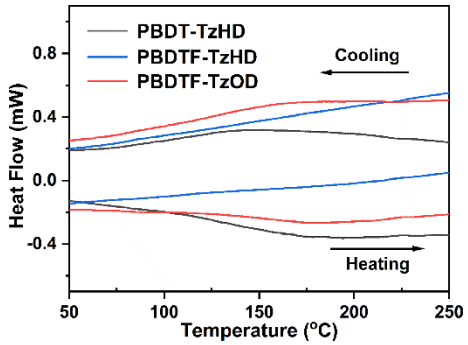

Figure S2 Differential scanning calorimetry traces for **PBDT-TzHD**, **PBDTF-TzHD**, and **PBDTF-TzOD**.

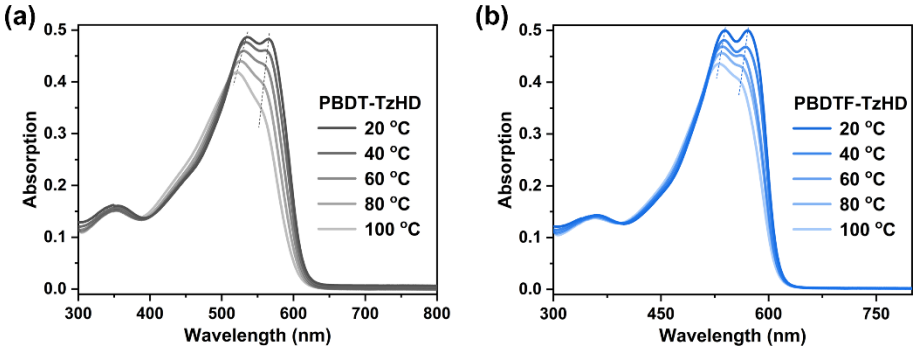

Figure S3 Temperature-dependent UV−vis absorption spectra of **PBDT-TzHD** (a) and **PBDTF-TzHD** (b) in chlorobenzene.

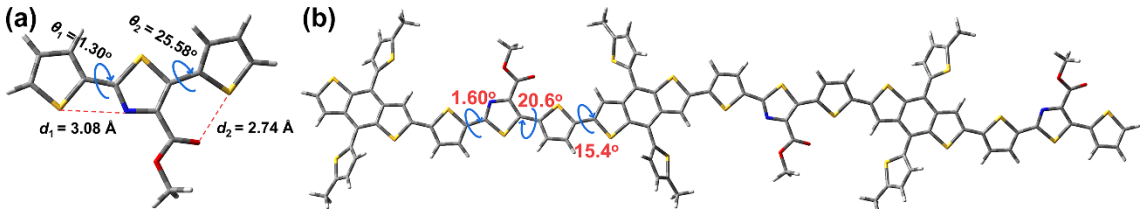

Figure S4 The geometry-optimized structure of TzTT-Me (a) and BDT-Tz (b)via DFT calculation.

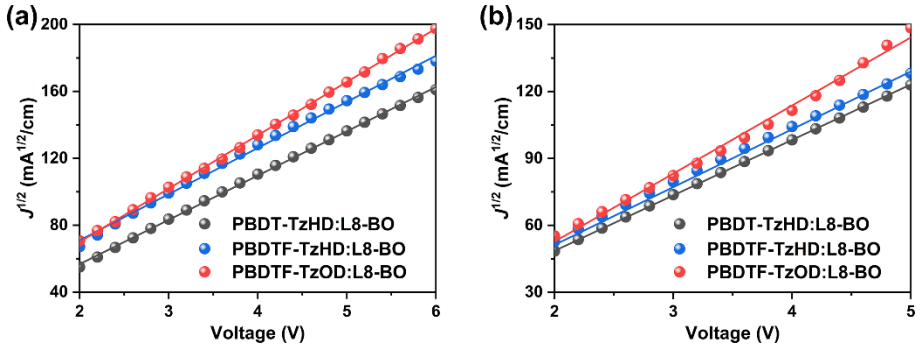

Figure S5 $J^{1/2}$–V characteristics for hole-only (a) and electron-only (b) devices based on **PBDT-TzHD**:L8-BO, **PBDTF-TzHD**:L8-BO, and **PBDTF-TzOD**:L8-BO.

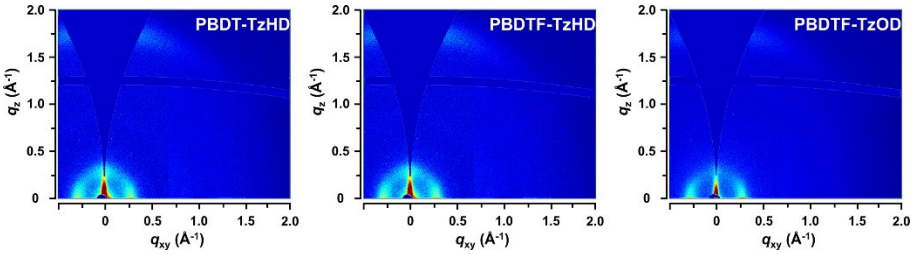

Figure S6 2D-GIWAXS patterns of the three neat films.

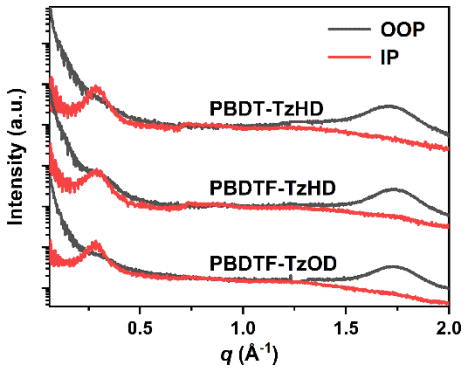

Figure S7 Line-cut profiles of three neat films.

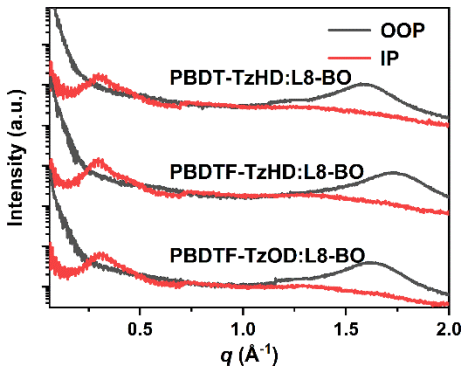

Figure S8 Line-cut profiles of three blend films.

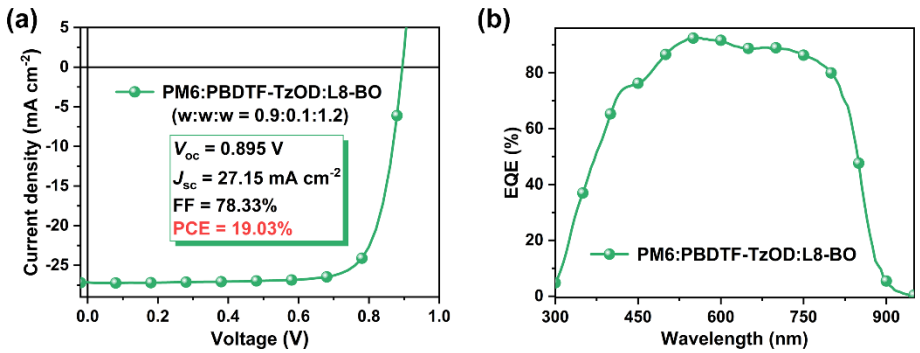

Figure S9 *J*–*V* curve (a) and EQE response (b) of the optimized ternary OSC device.

4 Supporting Tables

Table S1 The optimized dihedral angles (θ), orbital plane angles (α), bond lengths (d), and descriptors (S) for **TTz-Me**

Noncovalent interactions	θ [°]	α [°]	d [Å]	r_w[a] [Å]	Δd[b] [Å]	S
S···N	1.30	143.07	3.08	3.50	0.42	0.218
S···O	25.58	164.78	2.74	3.25	0.51	0.347

[a] r_w is the sum of van der Waals radii of two involved atoms. [b] Δd is defined as $r_w - d$.

Table S2 Photovoltaic parameters of PBDT-TzHD:L8-BO-based devices under different optimization conditions

D:A [w/w]	Additive [v/v]	TA Temperature [°C]	TA Time [min]	V_{oc} [V]	J_{sc} [mA·cm^{-2}]	FF [%]	PCE [%]
1:0.8				0.822	10.87	51.53	4.60
1:1				0.823	10.03	52.69	4.35
1:1.2				0.816	10.06	52.50	4.31
1:0.8	DIM (0.25%)			0.604	9.05	35.11	1.93
1:0.8	DPE (0.25%)			0.840	7.67	66.18	4.29
1:0.8	DIO (0.25%)			0.837	8.11	66.32	4.53
1:0.8	CN (0.25%)			0.695	10.68	28.43	2.12
1:0.8	None	120	1	0.703	8.52	26.82	1.61
1:0.8	None	120	3	0.822	9.37	49.28	3.80

Table S3 Photovoltaic parameters of PBDTF-TzHD:L8-BO-based devices under different optimization conditions

D:A [w/w]	Additive [v/v]	TA Temperature [°C]	TA Time [min]	V_{oc} [V]	J_{sc} [mA·cm^{-2}]	FF [%]	PCE [%]
1:0.8				0.899	20.63	58.36	10.82
1:1				0.893	21.02	58.41	10.96
1:1.2				0.890	20.49	56.22	10.25
1:1	DIM (0.25%)			0.875	18.43	55.96	9.03
1:1	DPE (0.25%)			0.883	12.08	56.94	6.07
1:1	DIO (0.25%)			0.870	19.43	52.64	8.90
1:1	CN (0.25%)			0.906	16.64	58.68	8.84
1:1	None	100	1	0.898	20.54	60.63	11.19
1:1	None	100	3	0.880	21.04	59.65	11.05
1:1	None	100	5	0.907	20.17	60.31	11.03

Table S4 Photovoltaic parameters of PBDTF-TzOD:L8-BO-based devices under different optimization conditions

D:A [w/w]	Additive [v/v]	TA Temperature [°C]	TA Time [min]	V_{oc} [V]	J_{sc} [mA·cm^{-2}]	FF [%]	PCE [%]
1:0.8				0.929	19.12	61.28	10.88
1:1				0.924	21.37	63.55	12.55
1:1.2				0.918	17.61	45.76	7.40
1:1	DPE (0.25%)			0.926	20.93	63.29	12.28
1:1	DIM (0.25%)			0.928	20.40	63.31	11.99
1:1	None	60	3	0.936	19.07	59.36	10.60
1:1	None	80	3	0.914	20.42	58.11	10.84
1:1	None	100	3	0.929	21.95	59.73	12.18
1:1	None	120	3	0.917	21.20	61.84	12.02
1:1	None	140	3	0.879	20.95	61.47	11.31
1:1	None	160	3	0.883	9.48	53.50	4.48

Table S5 Photovoltaic parameters of PM6:PBDTF-TzOD:L8-BO-based devices under different weight ratios

PM6:PBDTF-TzOD:L8-BO [w/w/w]	V_{oc} [V]	J_{sc} [mA·cm^{-2}]	FF [%]	PCE [%]
0:1.0:1.2	0.924	21.37	63.55	12.55
0.8:0.2:1.2	0.917	26.37	72.68	17.58
0.85:0.15:1.2	0.910	26.44	74.20	17.85
0.9:0.1:1.2	0.895	27.15	78.33	19.03
0.95:0.05:1.2	0.890	27.01	78.26	18.81
1.0:0:1.2	0.889	26.42	78.51	18.45

5 Geometric Coordinates

The Cartesian coordinates of all optimized geometries are now provided in the SI as follows:

TzTT-Me

C	1.5041	-0.3534	-0.0223
N	0.9669	0.8334	-0.0116
C	-0.4053	0.7865	-0.0036
C	-0.9836	-0.4826	0.0099
S	0.3218	-1.6650	-0.0341
C	-1.1513	2.0638	-0.0014
O	-0.3665	3.1121	0.3044
O	-2.3403	2.1714	-0.2498
C	-1.0296	4.3863	0.2943
C	2.9287	-0.6005	-0.0300
C	3.6059	-1.8017	-0.0178
C	5.0186	-1.6448	-0.0325
C	5.4003	-0.3284	-0.0556
S	4.0441	0.7494	-0.0593
C	-2.3406	-0.9950	0.0816
S	-3.7923	-0.1440	-0.4364
C	-4.7735	-1.5264	-0.1080
C	-4.0519	-2.5792	0.3938
C	-2.6731	-2.2775	0.4969
H	-0.2588	5.1145	0.5481
H	-1.4485	4.5951	-0.6945
H	-1.8381	4.4061	1.0309
H	3.1057	-2.7644	0.0030
H	5.7183	-2.4730	-0.0258
H	6.4063	0.0705	-0.0702
H	-5.8425	-1.4749	-0.2730
H	-4.4864	-3.5281	0.6879
H	-1.9396	-2.9767	0.8835

BDT-Tz

C	-25.0679	1.0803	0.0200
C	-25.5700	-0.2430	-0.1492
C	-24.6752	-1.3356	-0.2367
C	-23.3119	-1.0401	-0.1370
C	-22.8084	0.2837	0.0305
C	-23.7020	1.3770	0.1186
S	-26.3873	2.2432	0.1519
C	-27.5650	0.9600	-0.0081
C	-27.0107	-0.2699	-0.1543
S	-21.9981	-2.2088	-0.2553
C	-20.7923	-0.9176	-0.1151
C	-21.3758	0.3127	0.0266
C	-23.2381	2.7588	0.3078
C	-25.1348	-2.7200	-0.4256
S	-22.1886	3.2037	1.6498
C	-22.1904	4.8892	1.1948
C	-22.9707	5.0487	0.0848
C	-23.5717	3.8678	-0.4288
S	-26.1495	-3.1759	-1.7897
C	-26.1533	-4.8595	-1.3251
C	-25.3999	-5.0094	-0.1955
C	-24.8158	-3.8230	0.3257
C	-21.4359	5.9458	1.9390
C	-26.8839	-5.9238	-2.0820
C	-19.3834	-1.2355	-0.1569
C	-18.7865	-2.4288	-0.5251
C	-17.3761	-2.3944	-0.4588
C	-16.8802	-1.1756	-0.0389
S	-18.1756	-0.0462	0.2946
C	-15.5119	-0.7614	0.1449
S	-14.1486	-1.8364	-0.1783
C	-13.0326	-0.5620	0.3144

C	-13.7961	0.5610	0.6486
N	-15.1567	0.4246	0.5558
C	-13.2542	1.8631	1.0927
O	-14.2063	2.6705	1.5899
O	-12.0798	2.1853	1.0190
C	-13.7419	3.9612	2.0171
C	-11.6205	-0.8821	0.3171
C	-11.1106	-2.1748	0.2406
C	-9.7080	-2.2431	0.1816
C	-9.1060	-0.9969	0.2077
S	-10.2961	0.2784	0.3417
C	14.7149	0.9089	-0.1437
C	14.2298	-0.4327	-0.1275
C	15.1398	-1.5166	-0.0621
C	16.4994	-1.1914	-0.0292
C	16.9845	0.1498	-0.0455
C	16.0747	1.2338	-0.1111
S	13.3872	2.0607	-0.2675
C	12.2041	0.7428	-0.3294
C	12.8046	-0.4860	-0.2458
S	17.8267	-2.3439	0.0958
C	19.0098	-1.0263	0.1583
C	18.4099	0.2024	0.0734
C	16.5210	2.6339	-0.1475
C	14.6934	-2.9167	-0.0258
S	17.6523	3.2087	-1.3679
C	17.5818	4.8487	-0.7729
C	16.7218	4.8999	0.2874
C	16.1123	3.6697	0.6547
S	13.5592	-3.4904	1.1920
C	13.6281	-5.1298	0.5961
C	14.4899	-5.1818	-0.4628
C	15.1020	-3.9525	-0.8283

C	18.3646	5.9768	-1.3680
C	12.8408	-6.2563	1.1881
C	20.4177	-1.3230	0.2839
C	21.0123	-2.5312	0.6040
C	22.4225	-2.4675	0.6505
C	22.9208	-1.2114	0.3656
S	21.6291	-0.0812	0.0214
C	24.2901	-0.7611	0.3187
S	25.6526	-1.8495	0.5972
C	26.7667	-0.5027	0.3769
C	26.0079	0.6309	0.0817
N	24.6461	0.4677	0.0645
C	26.5575	1.9754	-0.2002
O	25.6179	2.9347	-0.1316
O	27.7247	2.2030	-0.4693
C	26.0866	4.2610	-0.4236
C	28.1808	-0.7749	0.5609
C	28.6845	-1.8700	1.2504
C	30.0953	-1.9743	1.2178
C	30.6702	-0.9599	0.4957
S	29.5080	0.1520	-0.1318
C	-5.6727	0.4962	-0.0121
C	-5.1759	-0.8256	0.1918
C	-3.8140	-1.1431	0.1839
C	-2.9137	-0.0697	-0.0267
C	-3.4105	1.2516	-0.2308
C	-4.7723	1.5695	-0.2232
C	-7.1032	0.5311	-0.0309
C	-7.6954	-0.6887	0.1673
S	-6.4963	-1.9748	0.3899
C	-1.4831	-0.1037	-0.0070
C	-0.8916	1.1163	-0.2039
S	-2.0903	2.4020	-0.4275

C	-5.2296	2.9522	-0.4223
C	-3.3564	-2.5258	0.3828
C	-4.8921	3.8134	-1.4365
C	-5.4884	5.0923	-1.2688
C	-6.2693	5.2476	-0.1586
S	-6.2771	3.7533	0.7438
C	-3.6930	-3.3870	1.3970
C	-3.0987	-4.6668	1.2277
C	-2.3202	-4.8230	0.1159
S	-2.3122	-3.3280	-0.7859
C	-7.0227	6.4698	0.2634
C	-1.5714	-6.0470	-0.3088
C	0.5184	1.4259	-0.2432
S	1.7217	0.1512	-0.3175
C	3.0223	1.3232	-0.3162
C	2.5315	2.6138	-0.2734
C	1.1212	2.6722	-0.2326
C	4.3889	0.8675	-0.3593
N	4.7389	-0.3885	-0.4054
C	6.0990	-0.5519	-0.4403
C	6.8674	0.6164	-0.4401
S	5.7573	1.9840	-0.3481
C	6.6363	-1.9292	-0.4794
O	5.6891	-2.8394	-0.7621
O	7.8028	-2.2228	-0.2756
C	6.1472	-4.2008	-0.7882
C	8.2813	0.9147	-0.5273
S	9.5952	-0.1995	-0.1644
C	10.7956	1.0397	-0.4498
C	10.2034	2.2390	-0.8069
C	8.8003	2.1653	-0.8486
F	-23.1558	6.2489	-0.5001
F	-25.2243	-6.2057	0.4007

F	-5.2992	6.0841	-2.1621
F	-3.2879	-5.6587	2.1206
F	16.4697	6.0424	0.9568
F	14.7408	-6.3244	-1.1330
H	-28.6195	1.2036	0.0196
H	-27.5899	-1.1791	-0.2514
H	-20.8030	1.2292	0.0968
H	-24.2022	3.8487	-1.3090
H	-24.2060	-3.7961	1.2203
H	-21.6012	6.9107	1.4512
H	-21.7683	6.0283	2.9807
H	-20.3576	5.7469	1.9474
H	-26.7264	-6.8853	-1.5848
H	-27.9628	-5.7312	-2.1190
H	-26.5251	-6.0107	-3.1145
H	-19.3510	-3.2967	-0.8479
H	-16.7421	-3.2364	-0.7163
H	-14.6288	4.4801	2.3816
H	-12.9986	3.8593	2.8131
H	-13.2919	4.5047	1.1812
H	-11.7420	-3.0565	0.2373
H	-9.1548	-3.1736	0.1149
H	12.2490	-1.4139	-0.2995
H	18.9651	1.1308	0.1251
H	15.4227	3.5647	1.4832
H	15.7923	-3.8477	-1.6563
H	18.1441	6.8936	-0.8138
H	19.4447	5.7959	-1.3143
H	18.1060	6.1433	-2.4205
H	13.0597	-7.1731	0.6332
H	13.0966	-6.4249	2.2409
H	11.7615	-6.0715	1.1323
H	20.4450	-3.4310	0.8152

H	23.0544	-3.3152	0.8939
H	26.4994	4.3097	-1.4355
H	25.2100	4.9029	-0.3333
H	26.8611	4.5615	0.2879
H	28.0497	-2.5703	1.7823
H	30.6548	-2.7587	1.7150
H	31.7249	-0.7845	0.3239
H	-7.6708	1.4344	-0.2160
H	-0.9161	-1.0078	0.1777
H	-4.2638	3.5491	-2.2781
H	-4.3205	-3.1226	2.2392
H	-6.8548	7.2623	-0.4715
H	-8.1012	6.2819	0.3241
H	-6.6919	6.8362	1.2425
H	-1.7404	-6.8398	0.4257
H	-1.9054	-6.4114	-1.2876
H	-0.4923	-5.8631	-0.3715
H	3.1693	3.4914	-0.2668
H	0.5607	3.5992	-0.1824
H	5.2649	-4.7972	-1.0219
H	6.9177	-4.3336	-1.5531
H	6.5610	-4.4865	0.1833
H	10.7659	3.1318	-1.0574
H	8.1756	3.0051	-1.1323

6 $^{1}H/^{13}C$ NMR and Mass Spectra of Key Intermediates and Final Products

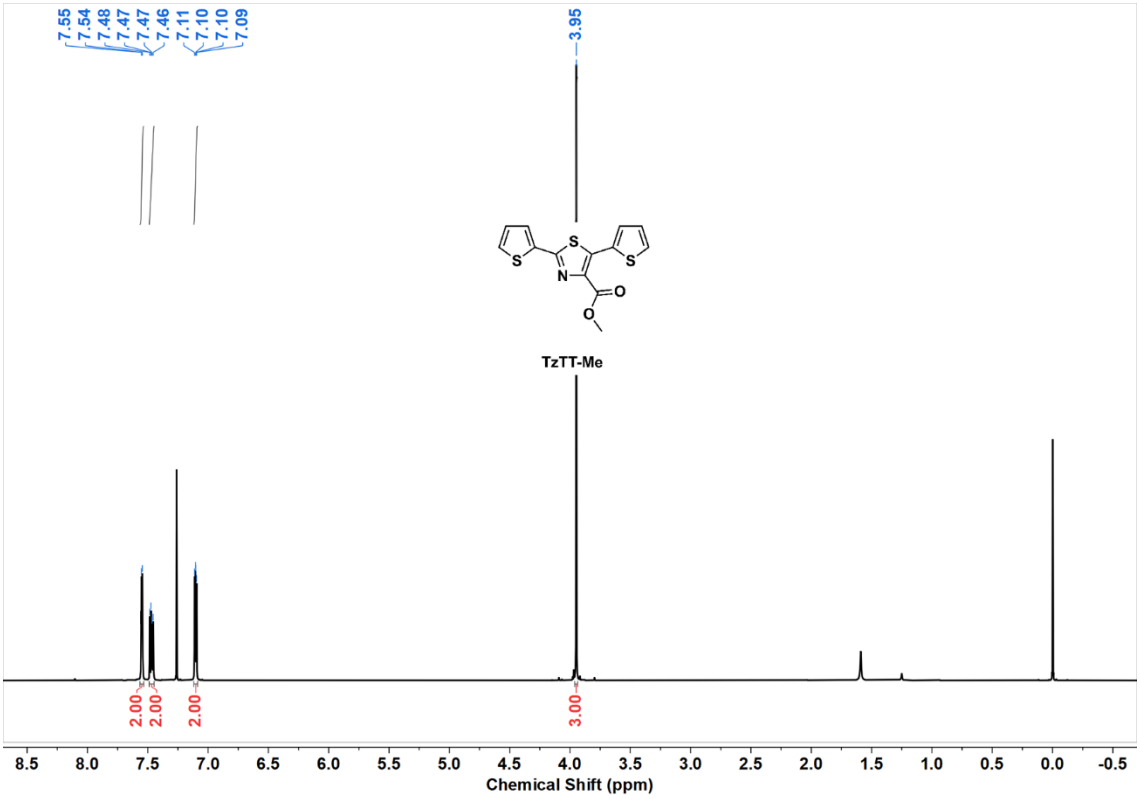

Figure S10 ^{1}H NMR (500 MHz) spectrum of TzTT-Me.

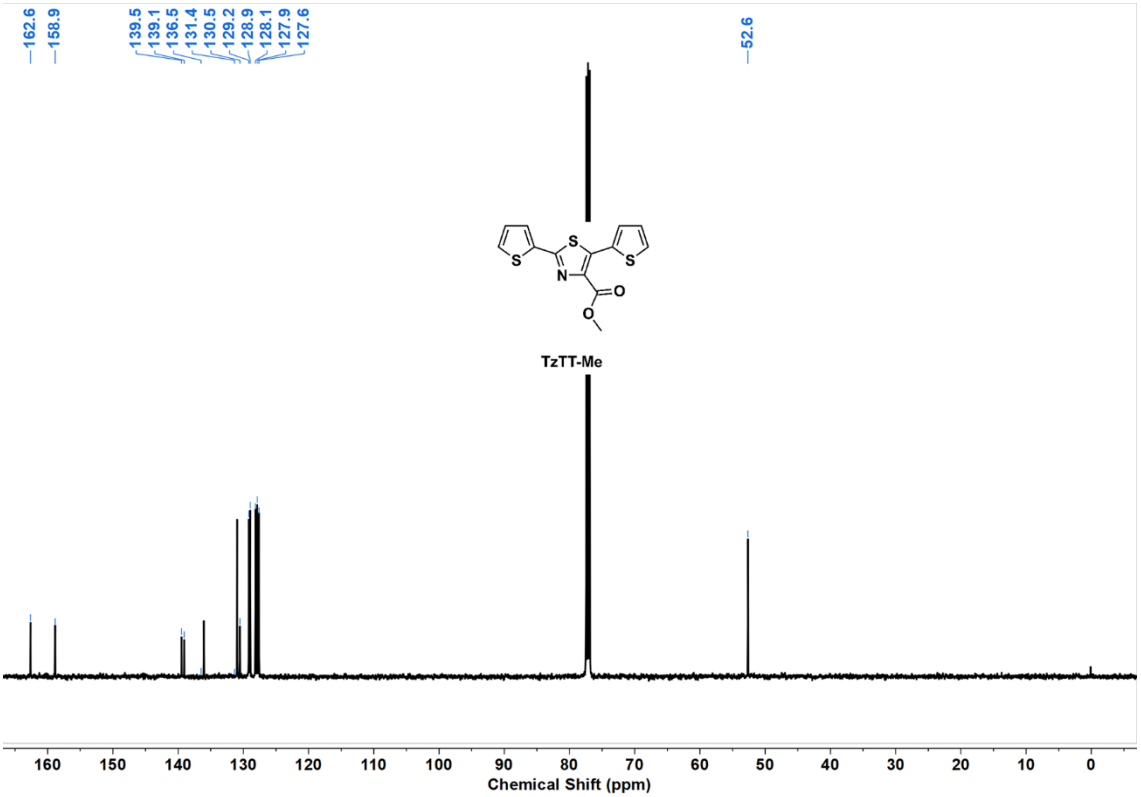

Figure S11 ^{13}C NMR (126 MHz) spectrum of TzTT-Me.

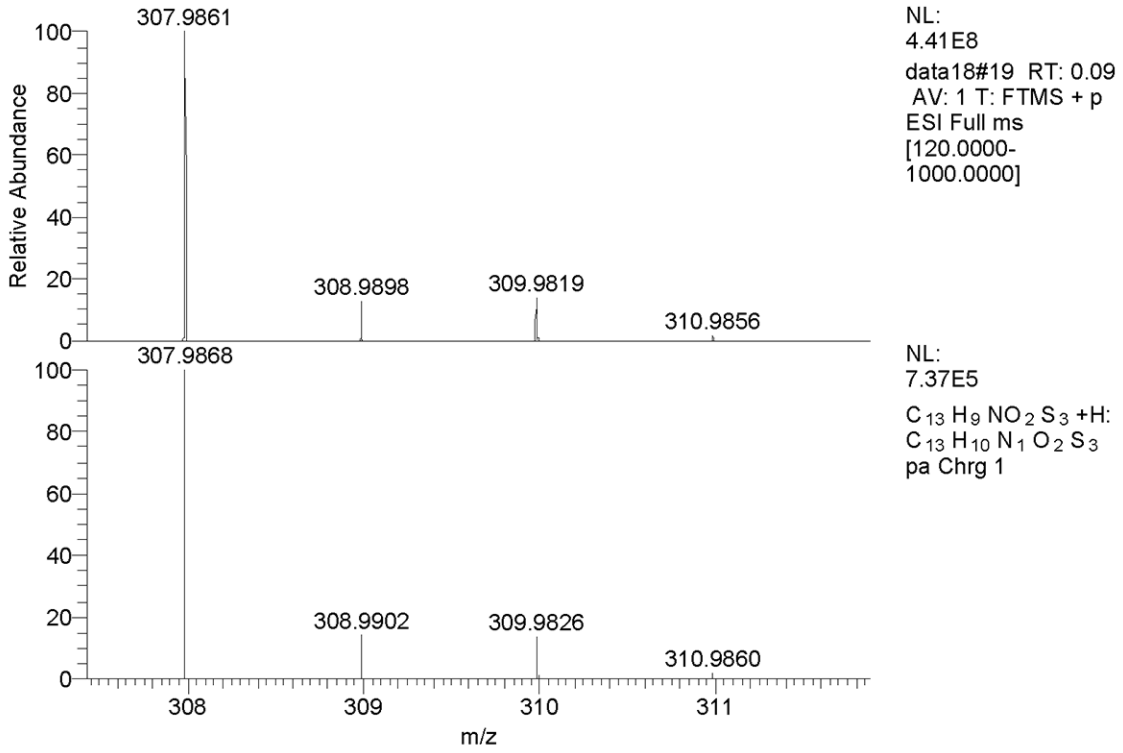

Figure S12 ESI mass spectrum of TzTT-Me.

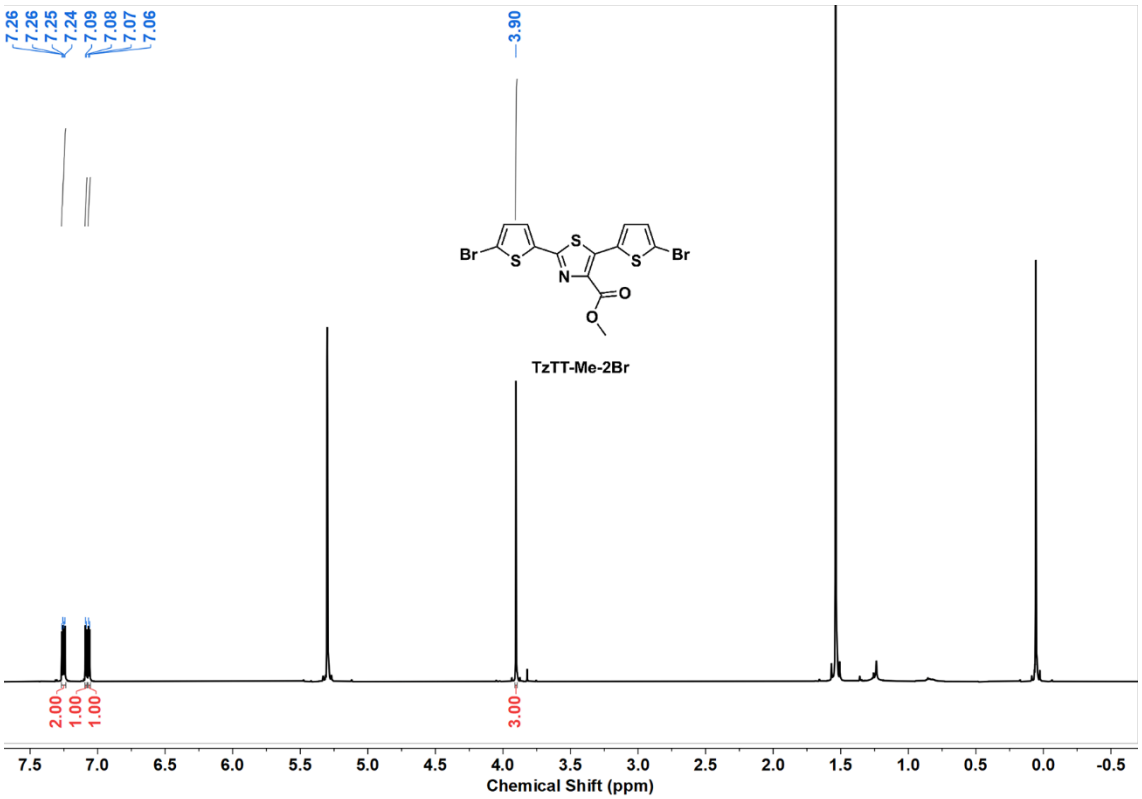

Figure S13 ^{1}H NMR (500 MHz) spectrum of TzTT-Me-2Br.

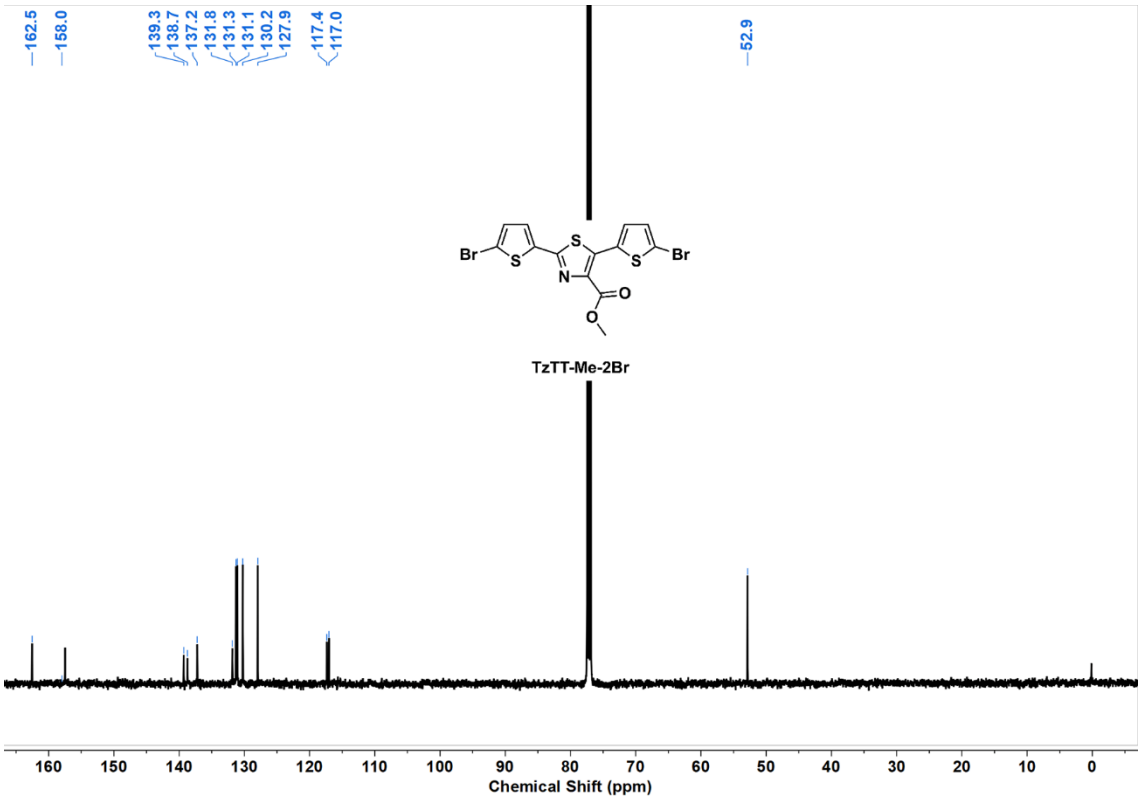

Figure S14 ^{13}C NMR (126 MHz) spectrum of TzTT-Me-2Br.

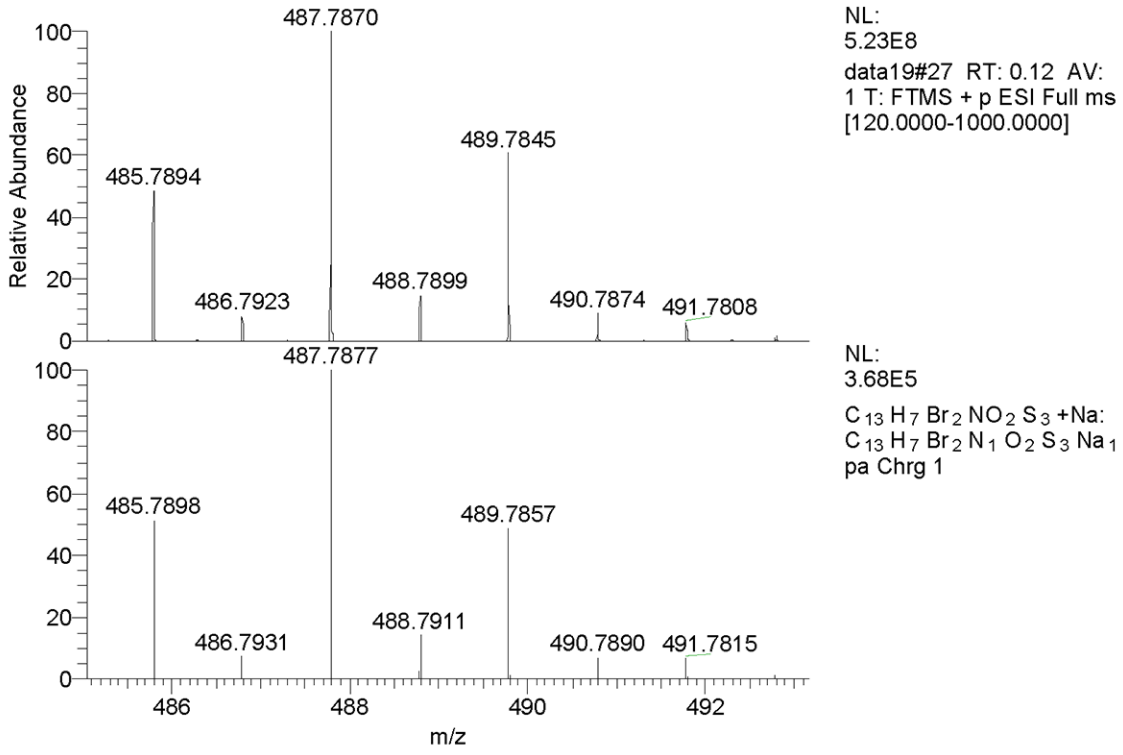

Figure S15 ESI mass spectrum of TzTT-Me-2Br.

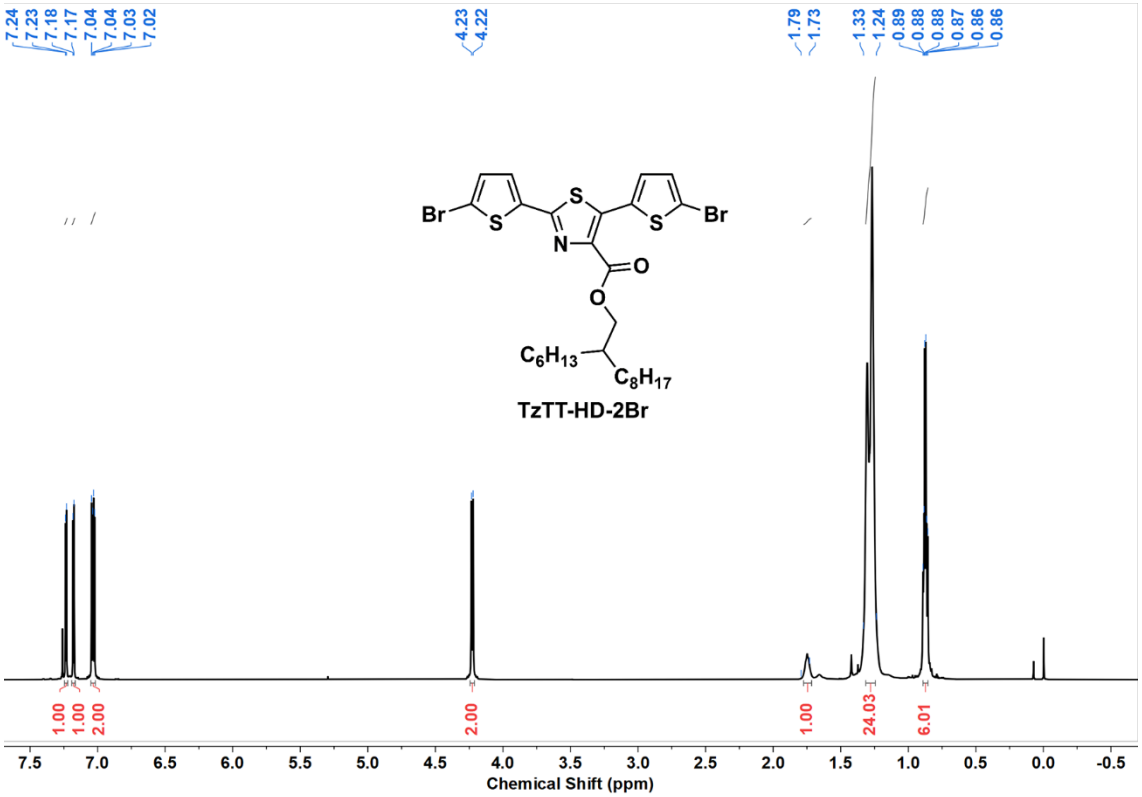

Figure S16 ^{1}H NMR (500 MHz) spectrum of TzTT-HD-2Br.

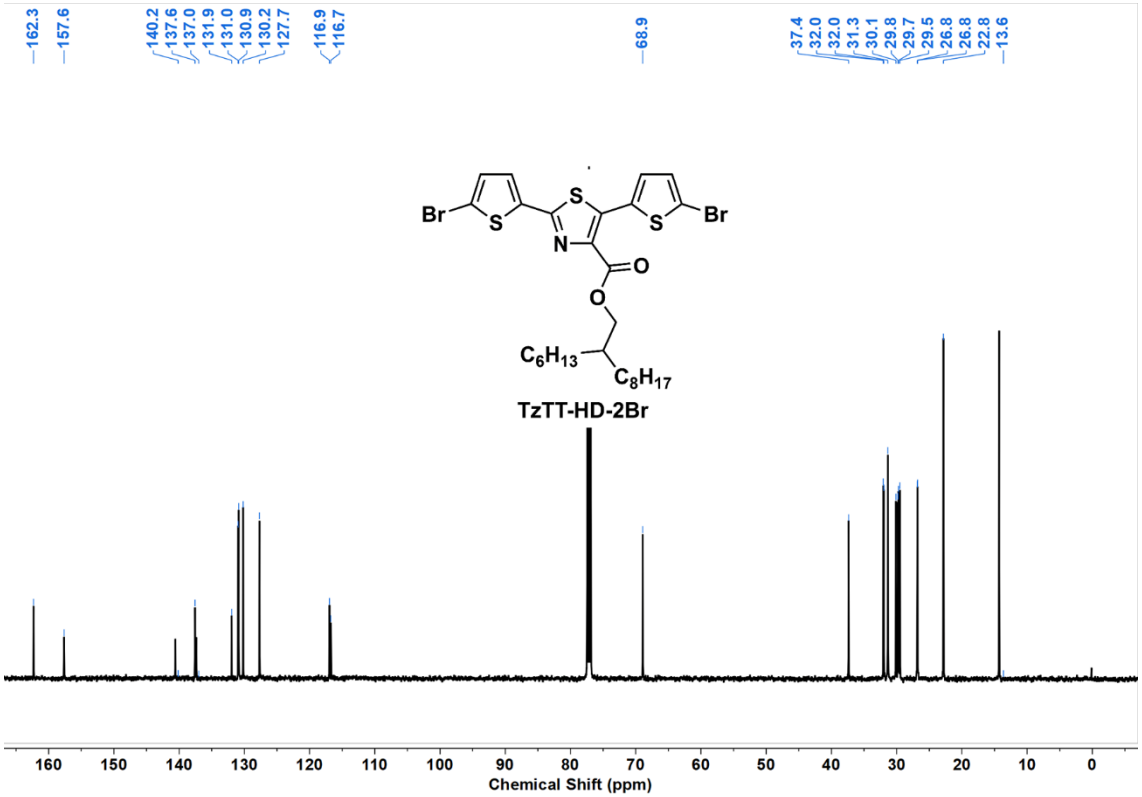

Figure S17 ^{13}C NMR (126 MHz) spectrum of TzTT-HD-2Br.

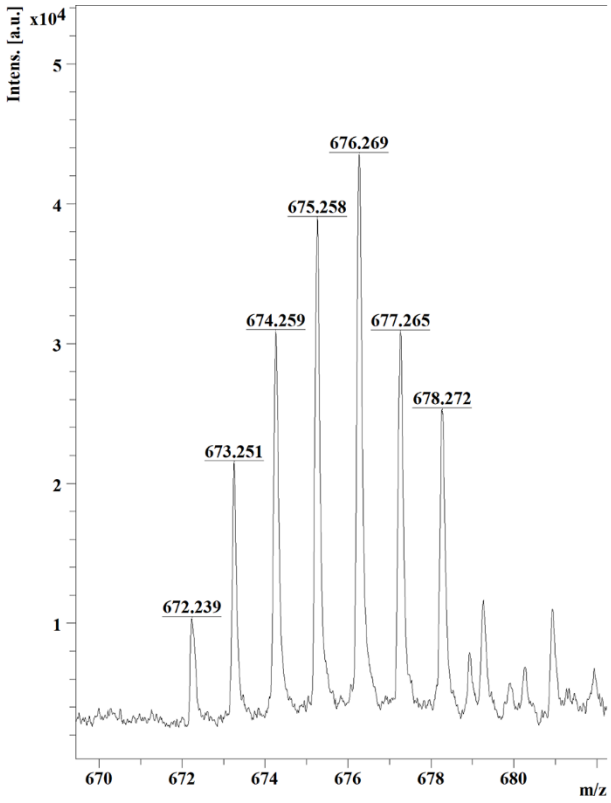

Figure S18 MALDI-TOF mass spectrum of TzTT-HD-2Br.

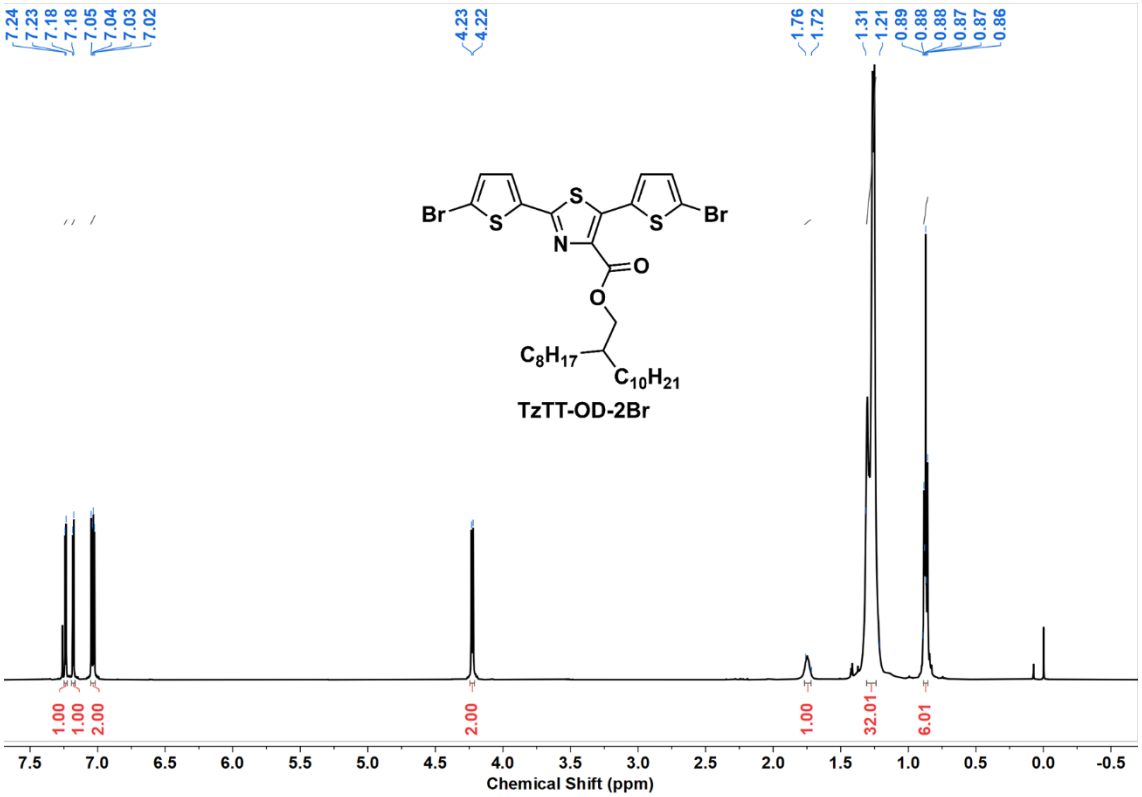

Figure S19 ^{1}H NMR (500 MHz) spectrum of TzTT-OD-2Br.

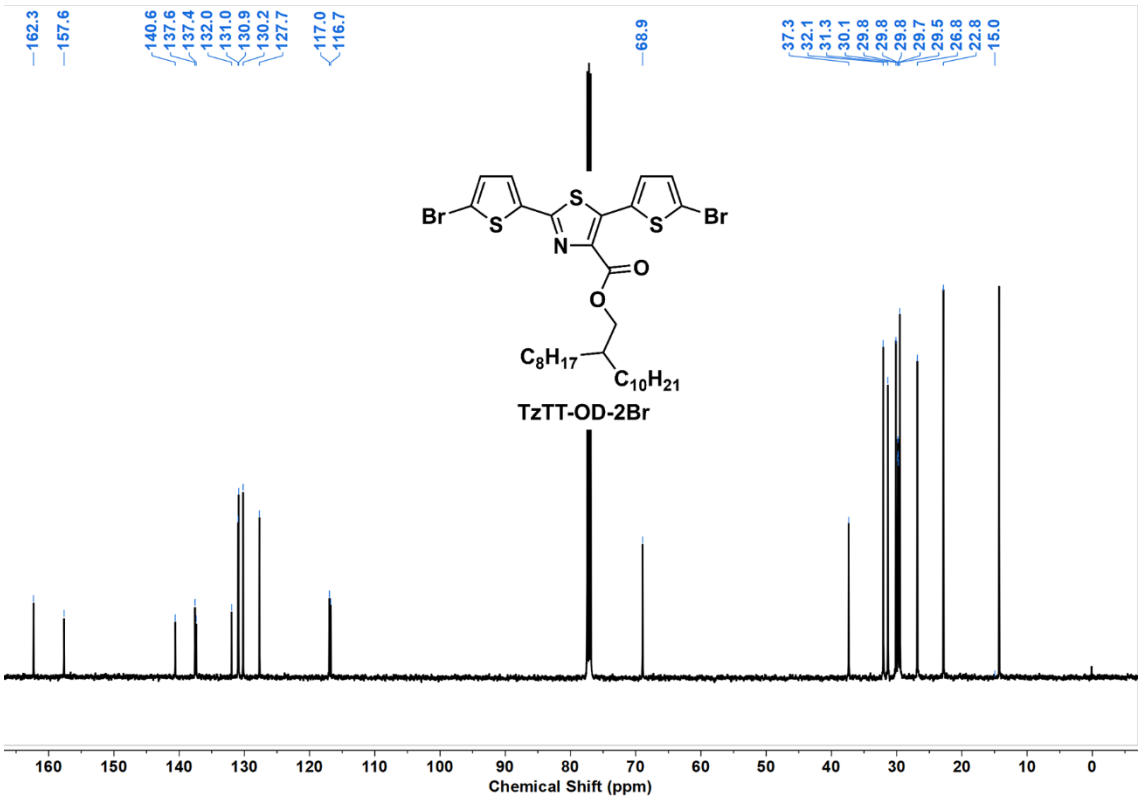

Figure S20 ^{13}C NMR (126 MHz) spectrum of TzTT-OD-2Br.

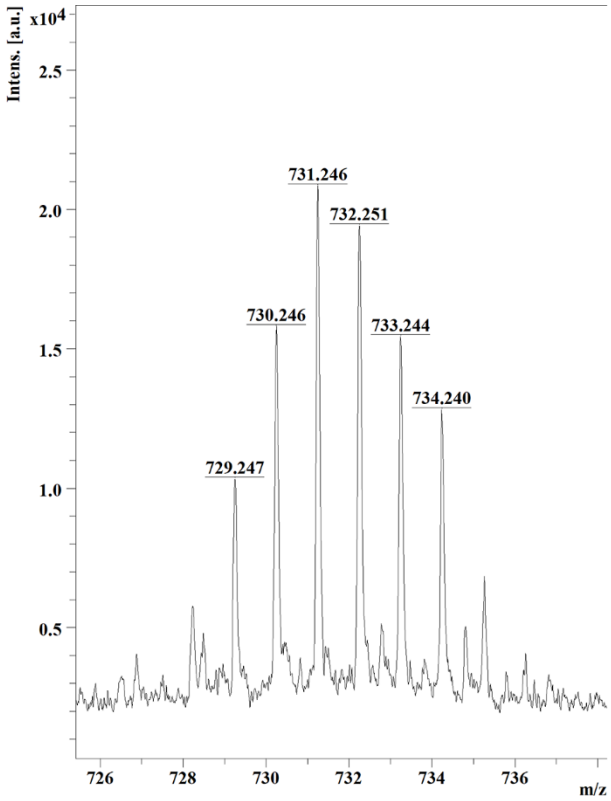

Figure S21 MALDI-TOF mass spectrum of TzTT-OD-2Br.

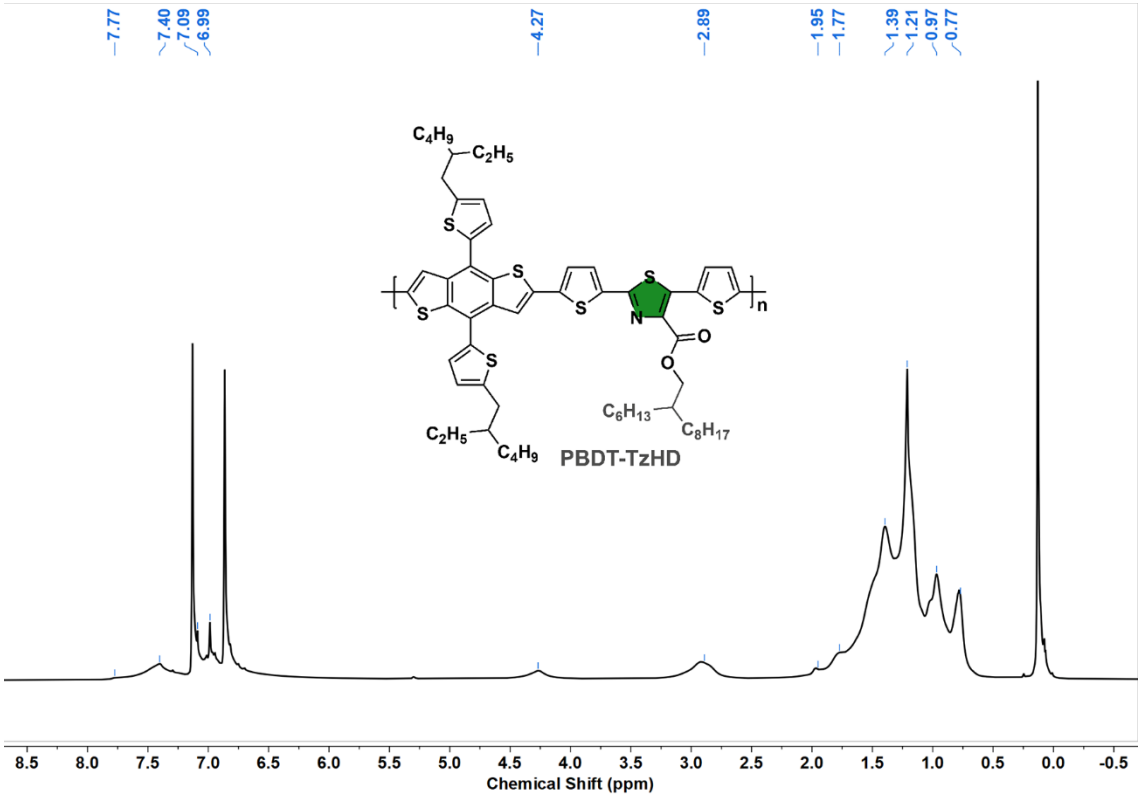

Figure S22 ^{1}H NMR (500 MHz) spectrum of PBDT-TzHD.

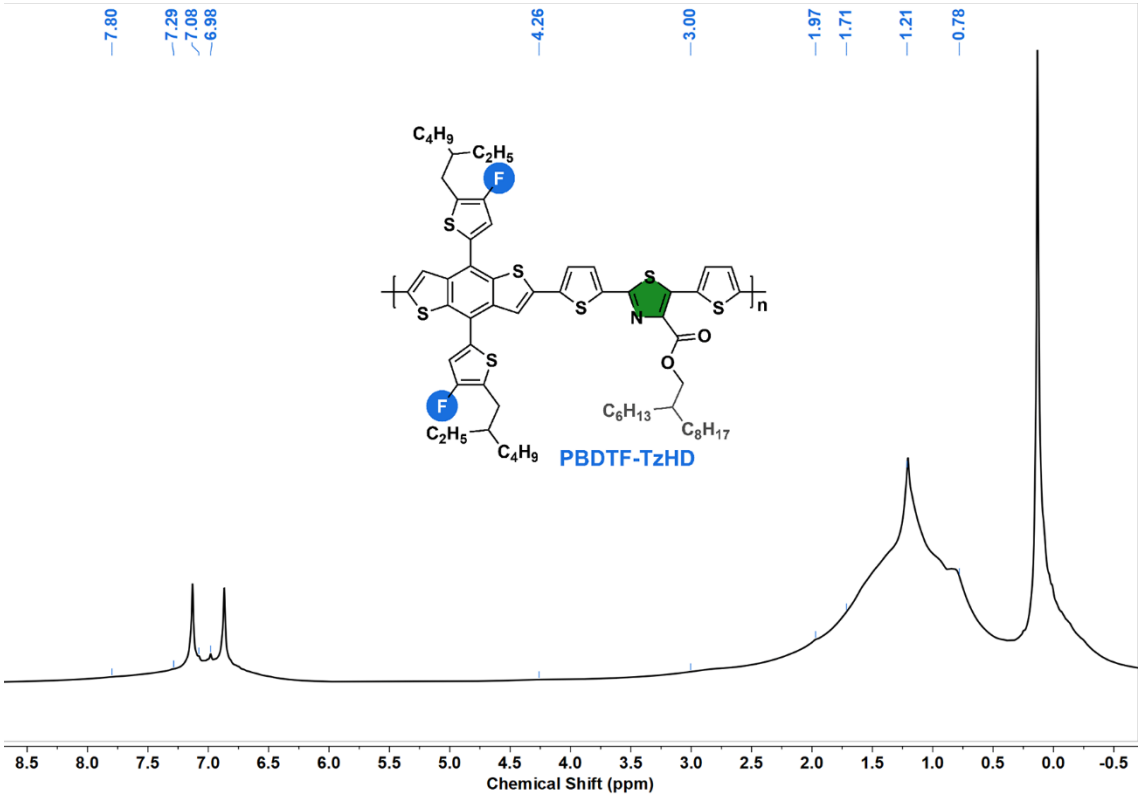

Figure S23 ^{1}H NMR (500 MHz) spectrum of PBDTF-TzHD.

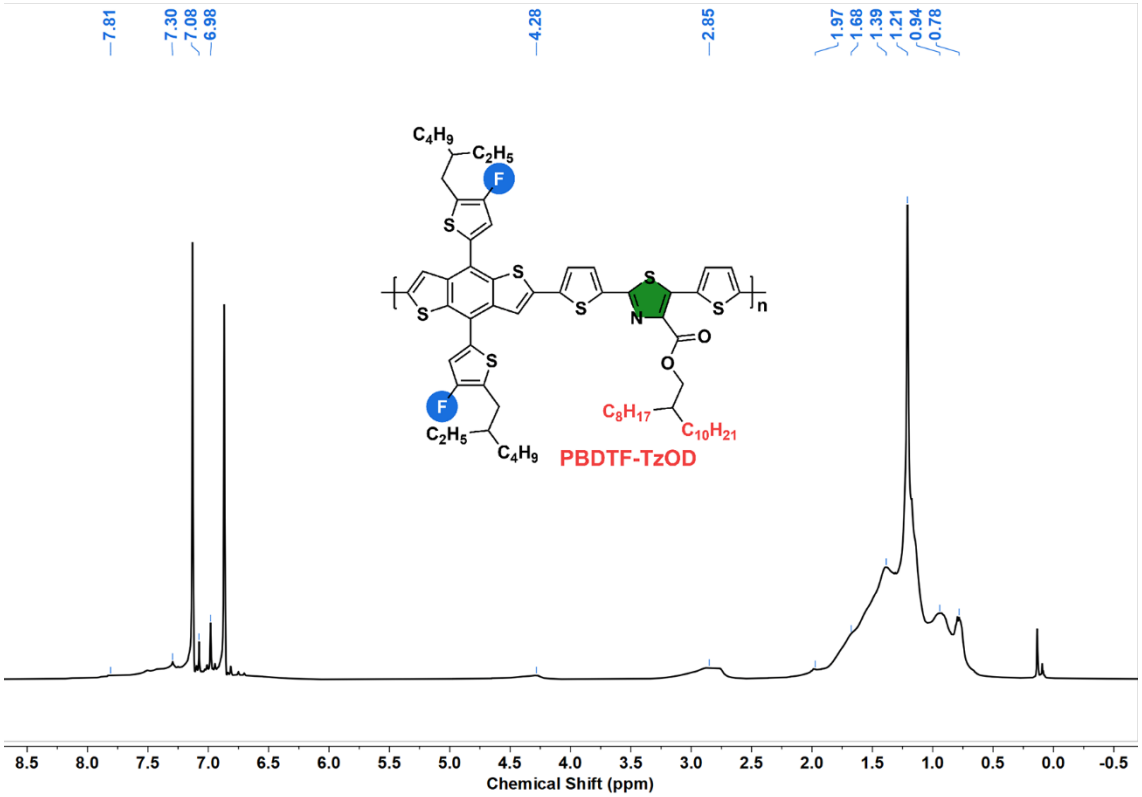

Figure S24 ^{1}H NMR (500 MHz) spectrum of PBDTF-TzOD.

References

[1] Frisch, M. J.; Trucks, G. W.; Schlegel, H. B.; Scuseria, G. E.; Robb, M. A.; Cheeseman, J. R.; Scalmani, G.; Barone, V.; Petersson, G. A.; Nakatsuji, H.; Li, X.; Caricato, M.; Marenich, A. V.; Bloino, J.; Janesko, B. G.; Gomperts, R.; Mennucci, B.; Hratchian, H. P.; Ortiz, J. V.; Izmaylov, A. F.; Sonnenberg, J. L.; Williams; Ding, F.; Lipparini, F.; Egidi, F.; Goings, J.; Peng, B.; Petrone, A.; Henderson, T.; Ranasinghe, D.; Zakrzewski, V. G.; Gao, J.; Rega, N.; Zheng, G.; Liang, W.; Hada, M.; Ehara, M.; Toyota, K.; Fukuda, R.; Hasegawa, J.; Ishida, M.; Nakajima, T.; Honda, Y.; Kitao, O.; Nakai, H.; Vreven, T.; Throssell, K.; Montgomery Jr., J. A.; Peralta, J. E.; Ogliaro, F.; Bearpark, M. J.; Heyd, J. J.; Brothers, E. N.; Kudin, K. N.; Staroverov, V. N.; Keith, T. A.; Kobayashi, R.; Normand, J.; Raghavachari, K.; Rendell, A. P.; Burant, J. C.; Iyengar, S. S.; Tomasi, J.; Cossi, M.; Millam, J. M.; Klene, M.; Adamo, C.; Cammi, R.; Ochterski, J. W.; Martin, R. L.; Morokuma, K.; Farkas, O.; Foresman, J. B.; Fox, D. J. Gaussian, Inc. *Wallingford CT* **2016**.

[2] Glendening, E. D.; Landis, C. R.; Weinhold, F. NBO 6.0: Natural bond orbital analysis program. *J. Comput. Chem.* **2013**, *34*, 1429-1437.

[3] Lu, T.; Chen, F. Multiwfn: A multifunctional wavefunction analyzer. *J. Comput. Chem.* **2012**, *33*, 580-592.

[4] Shen, Y.; Hosseini, A. R.; Wong, M. H.; Malliaras, G. G. How To Make Ohmic Contacts to Organic Semiconductors. *ChemPhysChem* **2004**, *5*, 16-25.